Origin of Multiple Melting Endotherms in a High Hard Block Content Polyurethane: Effect of Annealing Temperature

A. Saiani,*,† A. Novak,‡ L. Rodier,‡ G. Eeckhaut,§ J.-W. Leenslag,§ and J. S. Higgins||

School of Materials, The University of Manchester, Grosvenor Street, Manchester M1 7HS, U.K., Laboratoire de Thermodynamique des Solutions et des Polymères, Université Blaise Pascal / CNRS UMR 6003, 24, avenue des Landais, 63177 Aubière Cedex, France, Huntsman Polyurethanes, Everslaan 45, 3078 Everberg, Belgium, and Department of Chemical Engineering, Imperial College, Prince Consort Road, London SW7 2BY, U.K.

Received February 7, 2007; Revised Manuscript Received July 19, 2007

ABSTRACT: We have investigated the thermal behavior of a set of model linear thermoplastic polyurethanes (TPU) with a relatively high content of hard segments: from 50 to 100 wt %. The soft segment of these samples consists of poly(propylene oxide), end-capped with ethylene oxide (EO−PPO−EO), while the hard segment is composed of a 4,4′-methylenediphenylene isocyanate (4,4′-MDI) chain extended by a short diol chain, 2-methyl-1,3-propanediol (MP-Diol). In the present article, we have investigated the origin of the endotherms observed when samples are annealed below the glass transition of the hard segments T_{gHS}. The work was carried out using mainly differential scanning calorimetry (DSC) and small-angle and wide-angle X-ray scattering (SAXS and WAXS). The so-called "annealing endotherm", T_A, was observed 20−30 °C above the annealing temperature. The temperature and enthalpy of T_A were found to increase linearly with the logarithm of the annealing time. This endotherm was assigned to the relaxation (physical aging) of the interfacial materials. With increasing annealing temperature a change in the appearance of the hard phase glass transition, T_{gHP}, was observed. For long annealing times T_{gHP} is observed as an endotherm on the DSC thermographs. It is suggested that some of the hard segments undergo relaxation below T_{gHS} resulting in an enthalpy relaxation endotherm being present below or around T_{gHP}. An additional endotherm, $T_{M'}$, was observed as a shoulder at high temperature, just below the microphase mixing transition, T_{MMT}. This endotherm is thought to be due to the ordering during the phase separation process of the hard segment present in the mixed phase. Finally T_{MMT} was observed at all annealing temperature used suggesting that even at low annealing temperatures phase separation occurs. The delay time before phase separation starts and the maximum absolute degree of phase separation reached are found to increase with increasing annealing temperature. Our results suggest that a "thermodynamic equilibrium" is reached for each annealing temperature at long enough annealing times.

Introduction

Thermoplastic polyurethanes (TPU) are linear block copolymers typically constructed of statistically alternating soft (SS) and hard (HS) segments. Because of their numerous industrial applications, these materials have received considerable attention. Many characterization techniques have been used to try to understand the relationship between chemical architectures, morphologies, and mechanical properties of TPUs.[1,2] Their versatile physical properties are usually attributed to their microphase-separated structure deriving from the thermodynamic incompatibility between the soft and hard segments.[3−5] One important and intriguing feature of many aromatic TPUs is the apparent multiple melting endotherms observed via differential scanning calorimetry (DSC). The structural origin of these transitions has been the subject of a number of investigations; nevertheless, their origin is still not fully understood.[3−14]

In order to cast some light on the thermal behavior of TPUs we have recently investigated the thermodynamic and structural properties of a set of model linear TPUs with a relatively high content of hard segments: from 50 to 100 wt %. The soft segment of these samples consists of poly(propylene oxide), end-capped with ethylene oxide (EO−PPO−EO), while the hard segment is composed of 4,4′-methylenediphenylene isocyanate (4,4′-MDI), chain extended by a short diol chain 2-methyl-1,3-propanediol (MP-Diol). The use of MP-Diol in place of the commonly used 1,4-butanediol was an attempt to lower the temperature of the melting transitions to facilitate high temperature annealing studies.[15] In our previous work we have mainly focused on the thermal behavior of our samples when annealed at 120 °C, just above the hard segment glass transition (T_{gHS} = 119 ± 2 °C). We were able to assign the two high-temperature endotherms observed, T_M and T_{MMT}, to the melting of an ordered structure appearing in the hard segment phase during annealing and to the microphase mixing of the soft and hard segment respectively.[15] In order to confirm the thermodynamic findings we carried out a structural investigation. This work confirmed our previous results and allowed us to propose a structural model for the phase behavior of our samples. Above 65 wt % hard segment content a two-phase morphology was proposed for the melt-quenched samples one "pure" hard segment phase coexisting with a mixed phase with a hard segment content of 65 wt %. When the samples are annealed at 120 °C phase separation occurs in the mixed phase resulting in a phase-separated mesophase which has the same structure in all the samples.[16] This structural model allowed us to account for our small-angle X-ray (SAXS) results showing a scattering maximum for all the samples at the same momentum transfer, q, value (Figure

* Corresponding author. E-mail: a.saiani@manchester.ac.uk.
† School of Materials, The University of Manchester.
‡ Laboratoire de Thermodynamique des Solutions et des Polymères, Université Blaise Pascal/CNRS UMR 6003.
§ Huntsman Polyurethanes.
|| Department of Chemical Engineering, Imperial College.

10.1021/ma070332p CCC: $37.00
Published on Web 09/06/2007

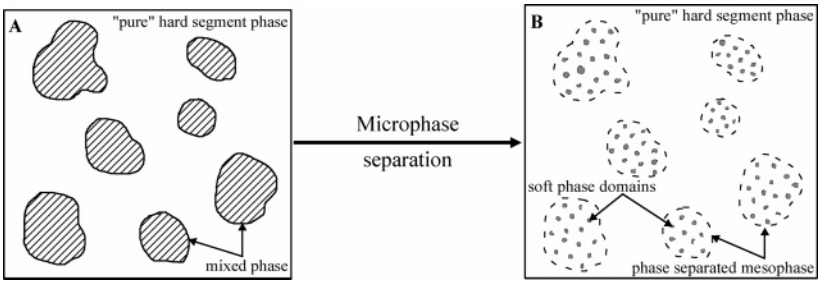

Figure 1. Schematic representation of the morphological model proposed for our sample with a continuous hard segment phase (see text and ref 16 for more details).

1, ref 16). A schematic representation of the morphology proposed is presented in Figure 1. The inversion point between a continuous mixed phase and a continuous hard phase morphology was estimated from the densities of the different phases to be around 74 wt % hard block content. The schematic diagrams presented in Figure 1 shows the situation where a continuous hard phase is present.

In this present article, we report on the further investigation of this set of samples focusing on samples with a hard segment content higher than 65 wt %. We have studied the effect of using different annealing temperatures on the thermal behavior of our samples and in particular on the multiple melting endotherms observed. The morphological origin of these endotherms is discussed. The work was carried out using mainly differential scanning calorimetry (DSC) and small angle and wide-angle X-ray scattering (SAXS and WAXS).

Experimental Section

Synthesis. All polyurethane samples were based on a prepolymer formulation. First, a master batch of prepolymer was prepared by reacting 1 mol of a commercial two-functional propylene oxide (PPO) ethylene oxide (EO), EO−PPO−EO, triblock copolymer (dried Daltocel F460 from Huntsman Polyurethanes: $M_w = 3700$/$M_n = 3083$) with 11.2 mol of 4,4′-methylenediphenylene isocyanate (4,4′-MDI) (Suprasec from Huntsman Polyurethanes). Second, a mixture of this prepolymer and 4,4′-MDI, so as to obtain the desired weight ratio between soft and hard segments, was slowly added to a preheated (85 °C) solution in dimethylacetamide (DMAC) of 2-methyl-1,3-propanediol (MP-Diol) in the presence of 0.25% catalyst (DABCO-S from Air Products).

The polymers were then isolated by precipitation. The cold PU/DMAC solution was added dropwise to a water (80)/ethanol (20) solution. The precipitated thermoplastic polyurethanes were filtered, washed with ethanol, and dried at room temperature. The dried powders were then ground at room temperature into smaller grains, washed for a second time with the ethanol/water mixture and finally dried in a vacuum oven at 120 °C. These TPU powders were compression molded into solid plaques at elevated temperature (160−200 °C depending on the hard segment content). A series of samples with a concentration of hard segment ranging from 65 to 95 wt % were synthesized.

The TPU samples were stored in a desiccator under dried atmosphere until used. Samples are designated according to the following nomenclature: PU−*XX*%HS where *XX* indicates the hard segment concentration by weight of the sample.

Differential Scanning Calorimetry. DSC measurements were performed using a Perking-Elmer Pyris 1 and a Mettler-Toledo 821^e/400 apparatus equipped with liquid nitrogen intra coolers. Experiments were performed under nitrogen atmosphere. Zinc and indium were used for a two-point calibration. Indium was used to calibrate the heat capacity. A 7−11 mg sample of material was cut out from the molded plates and introduced into an aluminum pan that was not hermetically sealed. The weight of the aluminum pan was measured before and after DSC experiments to ensure that there was no lost of material resulting from degradation. Figure 2

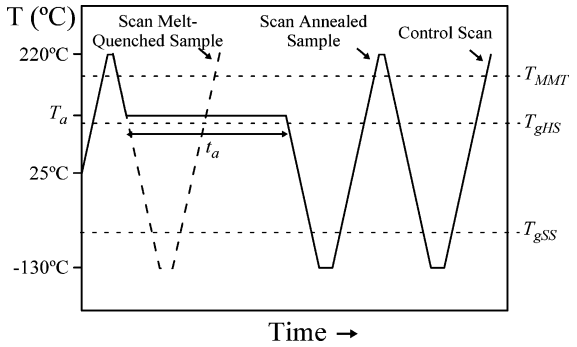

Figure 2. Thermal protocol used for the DSC experiments. The melt-quenched samples (dotted line) are melted 2 min at 220 °C, 40 °C above the highest melting endotherm T_{MMT}, and then quenched at low temperature, −130 °C, below the soft segment glass transition T_{gSS}. The DSC thermographs of the so-called "melt-quenched samples" are recorded during the following heating scan. The annealed samples (solid line) are melted for 2 min at 220 °C and then cooled directly to the annealing temperature, T_a, and kept at this temperature for an annealing time t_a. After annealing the samples are quenched at low temperature, −130 °C. The DSC thermographs of the so-called "annealed samples" are recorded during the following heating scan. After melting again for 2 min at 220 °C, the annealed samples are quenched at low temperature, −130 °C, and the so-called "control thermographs" are recorded during the following heating scan.

summarizes the DSC protocol used in this study for the so-called melt-quenched and annealed samples. The samples were initially melted at 220 °C and kept at this temperature for 2 min to clear all previous thermal history. All the thermal cycles were made directly in the DSC apparatus except for the very long annealing time experiments ($t_a > 8$ h) for which an oven pre-set at the annealing temperature was used. No significant difference was observed in the thermographs obtained for samples annealed the same time at the same temperature in the oven or directly in the DSC apparatus. If no other indications are given it as to be assumed that the DSC cycles were carried out at 20 °C min^{-1}. From all thermographs presented in this study, a baseline, obtained by running an empty pan under the same conditions as the sample, was subtracted, and for comparison purposes, all the thermographs were normalized by the weight of the sample. The analysis of the thermographs was carried out with the Perkin-Elmer Pyris Manager 2.04 software and the Mettler-Toledo QStar Software furnished with the instruments. For the endotherms the transition temperature was taken at the maximum of the peak and for the glass transition at the midpoint.

Gel Permeation Chromatography. GPC was used to determine the molecular weights of the TPUs. Dilute solutions (0.2% of polymer) were prepared in tetrahydrofuran (THF) and stirred overnight. The solutions were filtered through a 0.2 μm polyamide filter. The measurements were performed by Rapra Technology Ltd. at 30 °C using a polystyrene calibration and therefore the molecular weights are given in polystyrene equivalent. The molecular weights and polydispersities of the samples are listed in Table 1.

Small-Angle X-ray Scattering. The SAXS experiments were performed on beamline BM2 at the European Synchrotron Radiation Facility (ESRF), Grenoble, France and on beamline 8.2 at the CCLRC Daresbury Laboratory Synchrotron Radiation Source

Table 1. Average Molecular Weights and Polydispersities in Polystyrene Equivalents of the TPU Samples

samples	hard segment vol fraction Φ_{HS}	M_w	M_n	M_wM_n	calcd av M_w of hard segment[a]	calcd av no. of MDI per hard segment[a]
PU-65%HS	0.60	38 200	12 500	3.1	6900	20
PU-75%HS	0.71	43 200	12 500	3.5	11 100	33
PU-80%HS	0.76	69 800	12 700	5.5	14 800	44
PU-85%HS	0.82	33 400	11 300	3.0	21 000	62
PU-95%HS	0.88	57 700	11 200	4.5		171[b]

[a] Calculated from Peeble's most probable distribution.[32,33] [b] Calculated directly from the measured molecular weight (M_w.)

(SRS), Warrington, U.K. For beamline BM2 the incident energy used was 15 keV corresponding to a wave length of 8.3×10^{-2} nm. A collimated beam was produced with a typical cross section of 0.1×0.3 mm^2 at the sample position. An evacuated flight tube was placed between the sample and the detector in order to reduce air scattering and absorption. Two-dimensional SAXS patterns were collected on a 2D CCD detector (ref TECCD1242 E1FG0 M) from Princeton Instruments presently Roper Scientific (further details are available on request at Roper Scientific). The sample to detector distance was ~ 1 m corresponding to a momentum transfer vector range of $0.2 < q$ (nm^{-1}) < 4.5, q being defined as $q = (4\pi/\lambda) \sin(\theta/2)$, λ and θ being, respectively, the wavelength and the scattering angle (further details are available on request at the ESRF). For beamline 8.2 a highly collimated beam was produced with a typical cross section of 0.3×4 mm^2 in the focal plane. An evacuated flight tube was placed between the sample and the detector in order to reduce air scattering and absorption. The SAXS data were collected on a multiwire quadrant detector with an opening angle of 70° and an active length of 0.2 m. The sample−detector distance was 3.5 m, corresponding to an available momentum transfer vector range of $0.1 < q$ (nm^{-1}) < 2.0 (further details are available on request at the CCLRC).

The samples for the SAXS experiments were prepared by cutting ~ 1 cm^2 samples from the molded plates. To erase all previous thermal histories, the samples were melted at 220 °C for 2 min, and then pressed at high temperature so as to achieve a sample thickness of ~ 1 mm. The desired thermal treatment was then applied to the samples. To collect the SAXS data, the sample were placed in a 1 mm thick stainless steel holder closed by two mica windows each 25 μm thick. A home-built aluminum heating stage allowing a temperature control of ± 1 °C was used. The scattering intensities obtained were corrected for the detector response, the dark current, the empty cell, the sample transmission and the sample thickness. The two-dimensional pictures were radially regrouped in order to obtain the one dimensionnal SAXS pattern. A Lupolen standard was used for the intensity normalization and a collagen sample for the momentum transfer vector, q, normalization.

Degree of Phase Separation. The degree of phase separation of block copolymers can be estimated from the one-dimensional scattering pattern through the calculation of the electron density variances regardless of the type of morphology. The degree of phase separation is usually defined as the ratio[17,18]

$$\overline{\Delta\rho_e^2}/\overline{\Delta\rho_c^2} \tag{1}$$

between the experimental electron density variance

$$\overline{\Delta\rho_e^2} = \Phi_{HP}\Phi_{SP}(\rho_{HP} - \rho_{SP})^2 \tag{2}$$

Φ_{SP}, Φ_{HP}, ρ_{SP} and ρ_{HP} being respectively the soft phase (SP) and the hard phase (HP) volume fractions and electron densities, and the calculated theoretical electron density variance assuming complete phase separation

$$\overline{\Delta\rho_c^2} = \Phi_{HP}^c\Phi_{SP}^c(\rho_{HP}^c - \rho_{SP}^c)^2 \tag{3}$$

Φ_{SP}^c, Φ_{HP}^c, ρ_{SP}^c, and ρ_{HP}^c being in this case the soft phase (SP) and the hard phase (HP) calculated theoretical volume fractions and electron densities respectively. We choose to compute electron densities based on a completely phase separated model, where the soft phase corresponds to the soft segments and the hard phase to the hard segments. The electron density variance assuming complete phase separation can be calculated using the soft segment (SS) and hard segment (HS) volume fraction (Φ_{SS},Φ_{HS}) and electron densities (ρ_{SS}, ρ_{HS}):

$$\overline{\Delta\rho_c^2} = \Phi_{HS}\Phi_{SS}(\rho_{HS} - \rho_{SS})^2 \tag{4}$$

For a polymer, if its mass density, ρ_m, is known, the electron density, ρ_e, can be calculated from the molar mass, M_u, and the numbers of electrons, N_{e^-}, of its repeat unit through

$$\rho_e = \frac{N_{e^-}}{M_u} \times \rho_m \tag{5}$$

In our case, the repeat unit taken for the hard segment was a MDI−MP−diol unit and for the soft segment a PO unit. For the soft segments, the pure polyol density (1.02 g cm^{-3}) was used, and for the hard segment, the density measured for the amorphous PU-100%HS sample (1.27 g cm^{-3}) was used.[16] We obtained for our hard segment an electron density of $\rho_{HS} = 0.680$ e$^-$ mol cm^{-3} and for the soft segment $\rho_{SS} = 0.563$ e$^-$ mol cm^{-3}.

The experimental electron density variance can be calculated for a two phase system from the one-dimensional scattering data using the Porod invariant Q through[17−20]

$$\overline{\Delta\rho_e^2} = \frac{Q}{2\pi^2 i_e N_A^2} \tag{6}$$

i_e being the Thompson's constant for the scattering from one electron (7.94×10^{-26} cm^2) and N_A the Avogadro's number (6.02×10^{23} mol^{-1}). Q is defined as[17,18]

$$Q = \int_0^\infty \frac{[I(q) - I_b(q)]}{H(q)} q^2\, dq \tag{7}$$

$I_b(q)$ being the background scattering due to thermal fluctuation, and $H(q)$ is a function which models the size and shape of the interfacial boundary between the two phases. For a sigmoidal shaped interface

$$H(q) = \exp(-\sigma^2 q^2) \tag{8}$$

the thickness of the interface E being related to σ through

$$E \cong \sqrt{2\pi}\sigma \tag{9}$$

For a sharp interface $E = 0$, $H(q) = 1$ and

$$Q = \int_0^\infty [I(q) - I_b(q)] q^2\, dq \tag{10}$$

The values of $I_b(q)$ and σ can be extracted from the scattering data using the Porod law, which gives the scattering intensity of a two-phase system at high q values[17,18]

$$I(q) = \frac{K_p}{q^4}\exp(-\sigma^2 q^2) + I_b(q) \quad (11)$$

K_p being the Porod constant. In the investigated q range the background intensity, I_b, can be considered constant. The values of K_p, σ, and I_b are then obtained by fitting the tail of the scattering curves.

Wide-Angle X-ray Scattering. WAXS experiments were carried out on a Philips X'Pert-APD (PW3710) $\theta/2\theta$ instrument equipped with a Cu (Kα' 0.154 nm) anode X-ray tube run under operating conditions of 40 mA and 50 kV. Samples were prepared by cutting ~1 cm^2 samples from the molded plates. To erase all previous thermal histories, the samples were melted at 220 °C for 2 min, and then pressed at high temperature so as to achieve a sample thickness of ~1 mm. The desired thermal treatment was then applied to the samples. The WAXS patterns were collected a room temperature overnight.

Results and Discussion

The thermal stability of our samples and the thermal protocol used to investigate them has been extensively discussed in our previous article. In this earlier work, a thermal protocol was established in order to melt and anneal the samples avoiding significant degradation.[15] The same protocol has been used for the present work (Figure 2). All the samples were first melted for 2 min at 220 °C (40 °C above the highest melting endotherm) and then quenched at low temperature. In Figure 3 are presented the thermographs obtained for the melt-quenched samples. These results are reminiscent of the results obtained in our previous work. For a detailed discussion on melt-quenched samples we refer the reader to ref 15. The main result deriving from our previous investigation that is of importance for the present discussion is that for a hard segment content higher than 65 wt % our melt-quenched samples present a two phase morphology, one "pure" hard segments phase coexisting with a mixed (hard + soft segments) phase with a hard segment content of 65 wt %. For PU-75%HS, PU-85%HS, and PU-95%HS samples a clear glass transition is detected around 120 °C (Figure 3), corresponding to the glass transition of the "pure" hard segment phase, T_{gHP}. (All the symbols used in the present article and their definitions have been listed in Table 2.) For PU-65%HS sample as expected no T_{gHP} is observed instead a careful examination of the thermograph reveals the presence of what could be a very broad glass transition between −30 and +70 °C. This broad glass transition is thought to correspond to the mixed phase glass transition, T_{gMP}. This kind of broadening has already been reported for TPUs[10] and semicrystalline polymers and is usually ascribed to a large variation in segmental mobility. In our previous work T_{gMP} was clearly observed in the same temperature range for a lower hard segment content sample PU-50%HS.[15] PU-65%HS is expected to have a single mixed phase morphology after melt-quenching.

The melt-quench state was used in our work as a starting point for all our annealing experiments. This allowed us to ensure that all annealing experiments were performed on samples that were in a similar thermodynamic state. It also allowed us to check the reproducibility of our experiments. After each annealing experiment samples were again melted at 220 °C and quenched (Figure 2). The thermographs obtained on the subsequent scan were the same as the ones obtained for the so-called "melt-quenched" samples (Figure 3). Annealing experiments were also repeated twice on the same sample and the same results were obtained provided that the sample had been melt-quenched as described above prior each annealing experiment. These control experiments confirmed the validity

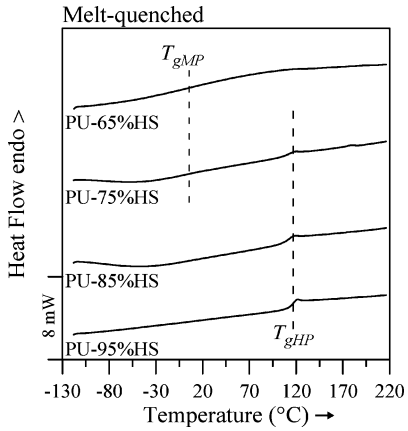

Figure 3. DSC thermographs obtained at 20 °C/min for the melt-quenched samples (for thermal protocol, see Figure 2).

Table 2. List of Symbols Used and Their Definitions

symbol	definition
T_a	annealing temperature
t_a	annealing time
T_{MMT}	microphase mixing transition
T_M	melting transition (hard segments present in hard segment phase)
$T_{M'}$	melting transition (hard segments present in mixed phase)
T_A	annealing endotherm
T_{gSS}	soft segment glass transition
T_{gHS}	hard segment glass transition
T_{gSP}	soft phase glass transition
T_{gHP}	hard phase glass transition

of the thermal protocol used in our work to erase the thermal histories of our samples. They also confirm that our protocol does not induce significant degradation of the samples. For a more extensive and detailed discussion of the thermal protocol used and the degradation of our samples, we refer the reader to ref 15.

Isochronal Annealing. In this section, we will discuss the effect of annealing the samples for 96 h at four different annealing temperatures (T_a): 60, 90, 120, and 160 °C. For comparison purposes, all the thermographs obtained have been presented together in Figure 4. All the characteristic values (enthalpies, temperatures, heat capacity changes) for all the transitions observed for the annealed as well as the melt-quenched samples have been summarized in Table 3.

We will first discuss the results obtained by annealing our samples at 120 and 160 °C (Figure 4, parts c and d), i.e. above T_{gHS} the glass transition of the hard segment. As mentioned earlier when annealed above T_{gHS} samples undergo phase separation. This is confirmed by the presence on PU-65%HS and PU-75%HS thermographs of a glass transition at low temperature, around −65 °C, corresponding to the glass transition of the soft phase, T_{gSP}. The glass transition of the pure soft segment used in these materials was found to be $T_{gSS} = -73 \pm 2$ °C. The difference between T_{gSP} and T_{gSS} can partly be accounted for by a mobility restriction effect due to the anchoring of the soft segments to the hard blocks.[11] In our previous work the glass transition of EO−PPO−EO end-capped at both ends with a single 4,4′MDI unit was found to be −64 ± 2 °C.[15] The values measured for T_{gSP} suggest the presence in our samples after annealing of an almost "pure" soft segment phase. The heat capacity change, ΔC_{pSP}, associated with T_{gSP} was found to be slightly larger for samples annealed at 160 °C (Table 3) suggesting that a larger amount of soft segments is residing in the soft phase. For PU-85%HS and PU-95%HS T_{gSP} was not detected. As discussed in our previous article, it is likely that due to the mobility restriction effect resulting from the

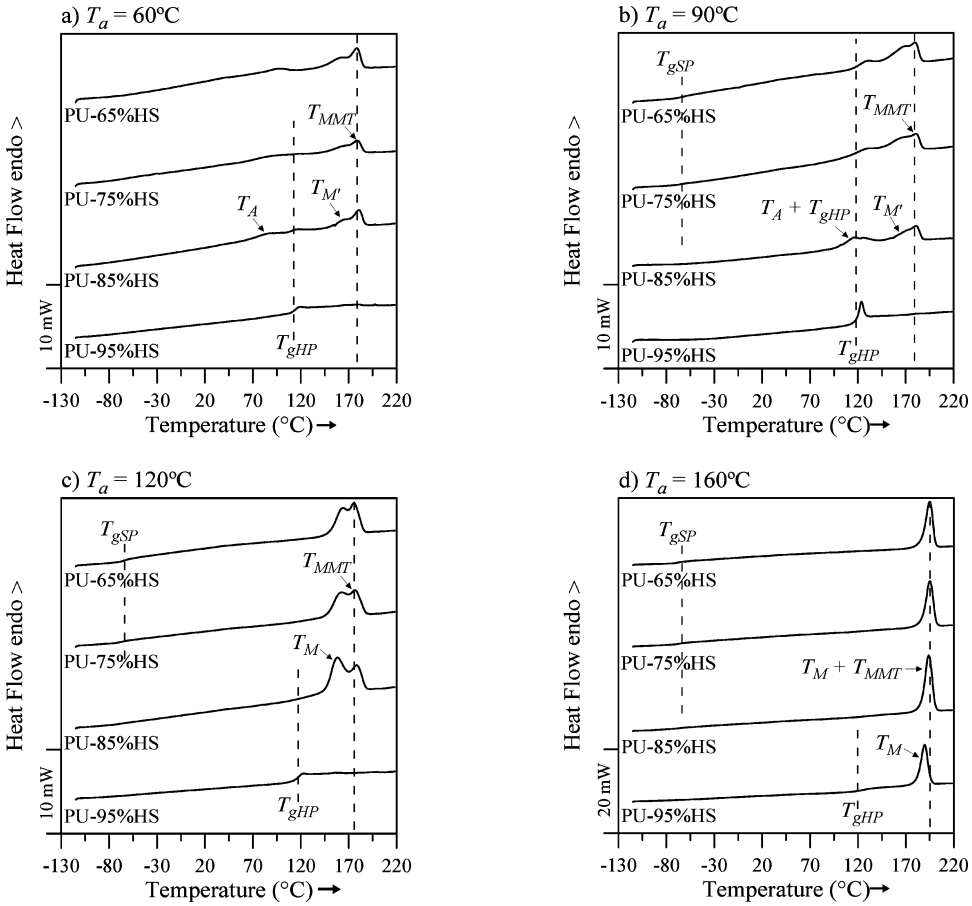

Figure 4. DSC thermographs obtained at 20 °C/min for samples annealed for 96 h at (a) 60, (b) 90, (c) 120, and (d) 160 °C (for thermal protocol, see Figure 2).

presence of the hard segments part of the soft segments do not present a glass transition and therefore do not contribute to T_{gSP}. The evaluation of the degree of phase separation from the values of ΔC_{pSP} is therefore not appropriate in our case.[15]

After annealing the samples at 120 °C two high-temperature endotherms are observed for all samples except PU-95%HS (Figure 4c). The effect of annealing our samples at 120 °C has been extensively discussed in our previous work. For a detailed discussion we refer the reader to refs 15 and 16. In this previous work, we have shown that the two endotherms observed can be assigned to the melting of an ordered structure developing in the hard phase during annealing, T_M, and to the microphase mixing of the soft an hard segments, T_{MMT}.

For PU-95%HS sample no high-temperature endotherms are observed. At this high hard block concentration, 95 wt %, we do not expect to be able to detect any microphase mixing transition, T_{MMT}. On the other hand, as we will see later, if an ordered structure were to develop in the hard phase during annealing a melting endotherm, T_M, should be observed. The absence of T_M suggests that for PU-95%HS sample the hard phase after 96 h of annealing is still amorphous. This is confirmed by the presence of a T_{gHP} with the same associated ΔC_{pHP} as for the melt-quenched samples (Table 3). It is probable that the annealing temperature used, 120 °C just above the glass transition of the hard segments, does not result in a sufficient increase in chain mobility to allow the ordering of the hard phase on the time scale investigated. On the other hand, when annealed at 160 °C, a clear melting endotherm is observed for PU-95%HS (Figure 4d) as well as a decrease in ΔC_{pHP} (Table 3) suggesting that at this higher annealing temperature an ordered structure develops in the hard phase during annealing. This was confirmed by wide-angle X-ray diffraction (WAXS) experiments where relatively weak diffraction peaks were observed suggesting the presence of a weakly ordered structure in the hard phase after annealing this sample at 160 °C. No such diffraction peaks were observed when annealing the sample at 120 °C.

A single melting endotherm is also observed for the lower hard segment content samples when annealed at 160 °C (Figure 4d). For these samples we expect to be able to detect both T_{MMT} and T_M. A number of authors have shown that the endothermic transitions observed via DSC in polyurethanes tend to shift toward higher temperatures and merge when the annealing temperature is increased.[8,9,12] This high-temperature endotherm observed for PU-65%HS, PU-75%HS, and PU-85%HS is therefore thought to correspond to ($T_M + T_{MMT}$). It is interesting to note that the temperature at which the endotherm is observed for these three samples is higher than for PU-95%HS (Table 3). This is in agreement with our previous suggestion that T_M only is observed for this latter sample which occurs at a lower temperature compared to T_{MMT}.

In parts a and b of Figure 4 are presented the thermographs obtained after annealing the samples for 96 h at 60 and 90 °C, respectively, i.e., below T_{gHS}, the glass transition of the hard segments. For all the samples except PU-95%HS, a high-temperature endotherm is observed around 180 °C corresponding to T_{MMT}. It suggests that even when annealed at these low temperatures, samples undergo phase separation. This is confirmed by the presence for PU-65%HS and PU-75%HS of a soft phase glass transition, T_{gSP}, around −65 °C when annealed at 90 °C (Figure 4b). T_{gSP} is found to be at the same temperature than for higher annealing temperatures (Table 3), suggesting a similar "purity" for the soft phase. The heat capacity change,

Table 3. Temperatures (°C), Enthalpies (J g^{-1}), and Heat Capacity Changes (J g^{-1} °C^{-1}) of Thermal Transitions

Melt-Quenched Samples (Figure 3)

samples	T_{gSP}	ΔC_{pSP}	T_A	T_{gHP}	ΔC_{pHP}	$T_{M'}$	T_{MMT}	ΔH_{Tot}
PU-65%HS	–	–	–	–	–	–	–	–
PU-75%HS	–	–	–	108.0	0.10	–	–	–
PU-85%HS	–	–	–	110.0	0.22	–	–	–
PU-95%HS	–	–	–	114.6	0.33	–	–	–

Annealed Samples: $T_a = 60$ °C and $t_a = 96$ h (Figure 4a)

samples	T_{gSP}	ΔC_pSP	T_A	T_{gHP}	ΔC_{pHP}	$T_{M'}$	T_{MMT}	ΔH_{Tot}
PU-65%HS	–	–	96.8	–	–	162.3	178.4	18.3
PU-75%HS	–	–	90.7[a]	*a*	*a*	163.8	178.7	11.3
PU-85%HS	–	–	85.5[a]	110.2[a]	*a*	165.8	180.7	10.5
PU-95%HS	–	–	–	113.8	0.31	–	–	–

Annealed Samples: $T_a = 90$ °C and $t_a = 96$ h (Figure 4b)

samples	T_{gSP}	ΔC_pSP	T_A	T_{gHP}	ΔC_pHP	$T_{M'}$	T_{MMT}	ΔH_{Tot}
PU-65%HS	−65.0	0.05	131.3	–	–	169.0	179.7	19.9
PU-75%HS	−64.6	0.00	131.5[a]	*a*	*a*	168.4	180.7	17.2
PU-85%HS	–	–	123.5[a]	110.4[a]	*a*	168.3	180.7	11.7
PU-95%HS	–	–	–	117.3	0.30	–	–	–

Annealed Samples: $T_a = 120$ °C and $t_a = 96$ h (Figure 4c)

samples	T_{gSP}	ΔC_pSP	T_A	T_{gHP}	ΔC_pHP	$T_{M'}$	T_{MMT}	ΔH_{Tot}
PU-65%HS	−65.5	0.08	–	–	–	164.1	175.4	28.5
PU-75%HS	−64.3	0.02	–	–	–	162.8	176.8	29.8
PU-85%HS	–	–	–	–	–	158.1	178.4	33.1
PU-95%HS	–	–	–	116.3	0.33	–	–	–

Annealed Samples: $T_a = 160$ °C and $t_a = 96$ h (Figure 4d)

samples	T_{gSP}	ΔC_pSP	T_A	T_{gHP}	ΔC_pHP	$T_{M'}$	T_{MMT}	ΔH_{Tot}
PU-65%HS	−67.0	0.12	–	–	–	195.0		31.1
PU-75%HS	−66.3	0.09	–	–	–	195.3		31.6
PU-85%HS	–	–	–	–	–	194.0		38.9
PU-95%HS	–	–	–	124.7	0.20	189.6	–	27.0

[a] Data estimated or not measured due to the overlap of T_A and T_{gHP}.

ΔC_{pSP}, associated with T_{gSP} is found to be decreasing with decreasing annealing temperature, suggesting a decrease in the amount of soft segment residing in the soft phase. For samples annealed at 60 °C, T_{gSP} could not be detected.

The presence of a phase-separated structure at low annealing temperature was confirmed by SAXS. In Figure 5 are presented the SAXS patterns obtained for the PU-65%HS sample after annealing for 72 h at 60, 90, 120, and 160 °C. As can be seen a characteristic scattering peak is observed for all the samples suggesting the presence in all of them of a phase-separated morphology. This is in agreement with our DSC results. No significant changes in the scattering patterns were observed for longer annealing times, suggesting that this sample has reached at these four temperatures its maximum degree of phase separation after 72 h annealing.[15,16] The position of the scattering maximum if found to be shifting toward smaller q values with increasing annealing temperature. As shown by our TEM picture (Figure 2, ref 16), no specific morphology is observed; therefore, as discussed in our previous article, we can extract from the position of the scattering maximum only a rough estimation of the interdomain distance, d_i, through the Bragg relation:[16,18,21]

$$d_i = \frac{2\pi}{q^*} \tag{12}$$

where q^* is the position of the scattering maxima. d_i was found to increase linearly with increasing annealing temperature (see the inset in Figure 5). In Table 4 are summarized the degree of phase separation estimated from our SAXS data. The methodology used to calculate the degree of phase separation has been explained in detail in our previous article[16] and has been summarized in the Experimental Section of this article. If a sharp interface model is used, the degree of phase separation is found to decrease with decreasing annealing temperature. In particular when annealed at 60 °C a significant decrease in the degree of phase separation is found. The degree of phase separation calculated using this model will from now on be referred to as "absolute degree of phase separation", as it is calculated in relation to the ideal case were the system is fully phase-separated; i.e., the two blocks belong to two distinct phases. In this model, the effect of the existence of an interface between soft and hard segments is not taken into account.

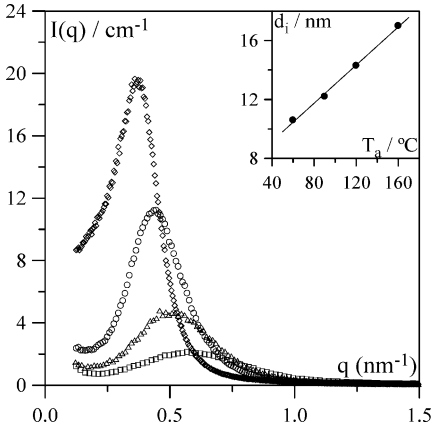

Figure 5. Intensity scattered $I(q)$ by PU-65%HS sample annealed for 96 h at 60 (□), 90 (○), 120 (△), and 160 °C (◇) vs momentum transfer q. Inset: interdomain distance d_i estimated through the Bragg relation (see text for details) vs annealing temperature T_a.

Table 4. Calculated and Experimental Electron Variances and Degrees of Phase Separation of PU-65%HS Samples

		sharp boundary ($E = 0$)		sigmoidal boundary [$E = (2\pi)^{1/2}\sigma$]		
annealing temp (T_a) (°C)	$\overline{\Delta\rho_c^2} \times 10^3$ (e^- mol cm^{-3})^2	$\overline{\Delta\rho_e^2} \times 10^3$ (e^- mol cm^{-3})^2	phase separation (%) $\overline{\Delta\rho_e^2}/\overline{\Delta\rho_c^2} \times 100$	$\overline{\Delta\rho_e^2} \times 10^3$ (e^- mol cm^{-3})^2	phase separation (%) $\overline{\Delta\rho_e^2}/\overline{\Delta\rho_c^2} \times 100$	boundary thickness E (nm)
160	3.28	1.53	47	1.77	54	1.1
120	3.28	1.58	48	1.96	60	1.2
90	3.28	1.40	43	1.83	56	1.5
60	3.28	0.96	29	1.94	60	1.7

The soft and hard segment being covalently linked a smooth interface between hard and soft domains is expected. If a sigmoidal interface model is used, the degree of phase separation is found to be constant and the interfacial thickness is found to increase with decreasing annealing temperature (Table 4). The degree of phase separation calculated using this latter model will be referred to as "relative degree of phase separation" as it is related to the relative purity of the two phases. It should also be noted that the temperature at which T_{gSP} is observed by DSC (Table 3) is related to the relative degree of phase separation as it is function of the purity of the soft phase. The fact that T_{gSP} is always found at the same temperature suggests a similar relative degree of phase separation in all the samples, in agreement with the SAXS results. On the other hand ΔC_{pSP} is related to the absolute degree of phase separation of the samples and the decrease in ΔC_{pSP} with increasing annealing temperature suggest an increase in the absolute degree of separation with increasing annealing temperature in agreement again with our SAXS results.

Two additional endotherms can be observed when annealing the samples at 60 and 90 °C (Figure 4a,b). T_A is observed at 20−30 °C above the annealing temperature and is usually referred to as the "annealing endotherm". The second endotherm, $T_{M'}$, is observed as a shoulder just below T_{MMT}. The origin of these two endotherms will be discussed in detail in the next

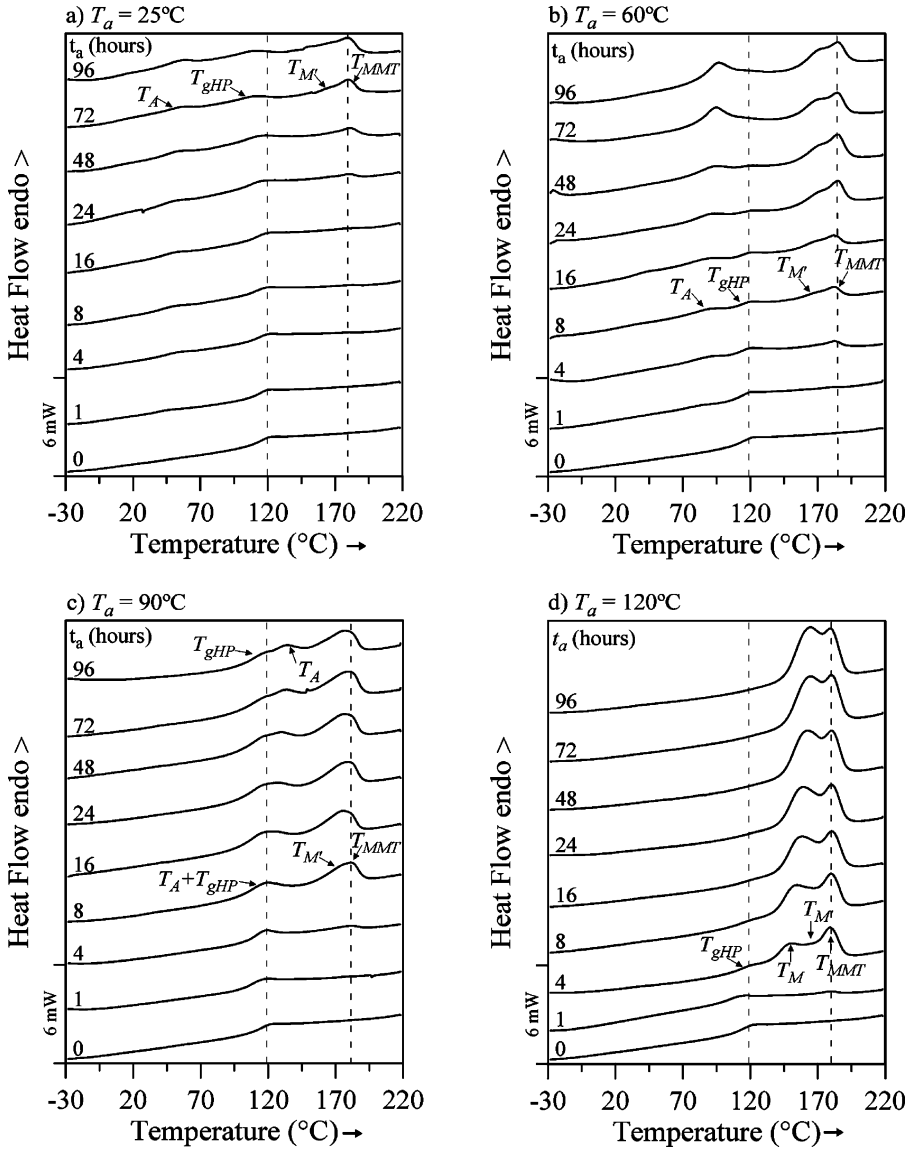

Figure 6. DSC thermographs obtained at 20 °C/min for PU-80%HS sample annealed at (a) 25, (b) 60, (c) 90, and (d) 120 °C as a function of annealing time, t_a.

section where the behavior of PU-80%HS sample has been investigated as a function of annealing time.

The hard phase glass transition, T_{gHP}, is difficult to observe clearly at low annealing temperature, except for PU-85%HS sample annealed at 60 °C, due to the overlapping with T_A (Figure 4, parts a and b). Nevertheless, the presence of T_{gHP} suggests, as expected, that the ordering of the hard phase is less pronounced for these low annealing temperatures (below T_{gHS}) than for high annealing temperatures (above T_{gHS}) where T_{gHP} is not observed (Figure 4, c and d). For PU-95%HS sample an "overshoot" can be observed at T_{gHP} when annealed at 90 °C.

Isothermal Annealing of the PU-80%HS Sample. In Figure 6, the thermographs obtained for PU-80%HS sample at four different annealing temperatures, $T_a = 25$, 60, 90, and 120 °C, are presented as a function of annealing times, t_a. When melt-quenched ($t_a = 0$, Figure 6), a single transition is detected corresponding to the glass transition of the hard segment phase, T_{gHP}. As discussed in the previous section, the PU-80%HS sample is expected to have a two-phase morphology after melt-quenching one "pure" hard segment phase coexisting with a mixed phase with a hard segment content of 65 wt %. When annealed, the mixed phase will undergo phase separation.

We will first discuss the origin on the transitions observed below and around T_{gHP}. In Figure 6a, the thermographs obtained when annealing a PU-80%HS sample at 25 °C are presented. The appearance and growth with increasing annealing time (t_a) of the so-called "annealing endotherm", T_A, around 45−50 °C can clearly be observed. The temperature as well as the associated enthalpy, ΔH_A, is found to increase linearly with log(t_a) (Figure 7). The same characteristic behavior for T_A was observed by other authors and in particular by Chen et al., who carried out a detailed investigation of the behavior of the annealing endotherm for 4,4′MDI/BDO-based polyurethanes.[7,22] This type of behavior is characteristic of enthalpy recovery endotherms also called in the literature enthalpy relaxation endotherms. When polymers are cooled below their glass transition temperature, T_g, they usually have not reached their equilibrium conformation. Below T_g, the relaxation times become extremely long, and polymer chains will rearrange on very long time scales. When polymers are annealed at a constant temperature for long times, the enthalpy relaxation related to the slow relaxation of the polymer chain toward its equilibrium conformation, also called physical aging, is recovered on the subsequent heating and is visible on the DSC thermograph as an endothermic peak. The key characteristic properties of these enthalpy recovery endotherms have been discussed and summarized by Hodge in a review article.[23] They are usually observed 20−30 °C above T_a, and the temperature and enthalpy of these endotherms are found to increase linearly with log(t_a) at constant annealing temperature for relatively short annealing times. For homopolymers usually enthalpy recovery endotherms are observed when annealed close to their T_g. They are observed in most cases as "overshoots" just above T_g, or alternatively, they can be observed as shoulders just below T_g.[23−25] A characteristic example of enthalpy recovery endotherm can be seen for PU-95%HS sample when annealed at 90 °C (Figure 4b). At lower annealing temperature no enthalpy recovery endotherm is observed neither above nor below T_{gHP} for this sample (Figure 4a).

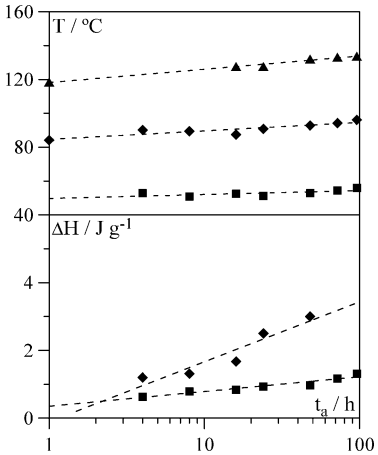

Figure 7. Temperatures and enthalpies of the annealing endotherm T_A (see Figure 7) vs the logarithm of the annealing time t_a for PU-80%HS sample when annealed at 25 (■), 60 (◆), and 90 °C (▲). Upper graph: temperatures. Lower graph: enthalpies.

In the case of PU-80%HS sample when annealing at 25 °C T_A is observed ∼80 °C below T_{gHP} suggesting that T_A does not originate from the physical aging of the "pure" hard segments phase. As enthalpy recovery endotherms are not observed by definition for annealing temperatures above T_g, T_A does not originate from the soft phase. The only possible origin for T_A is the interface between the soft and hard phases. It is expected for this type of segmented block copolymers to find a significant amount of material in the interfacial regions, and T_g is expected to vary continuously between T_{gSP} and T_{gHP} across the interface.[26−28] When annealing at low temperatures, the material in the interface region with a glass transition just above T_a will undergo physical aging which will result in the presence of an enthalpy recovery endotherm on the subsequent heating. This type of behavior was already observed by Quan et al. for a set of polystyrene hompolymer styrene−isoprene-styrene block copolymer blends. These authors observed the presence of enthalpy recovery endotherms 20−30 °C above T_a when annealing their system at any temperature in between the glass transitions of the two polymers. They assigned the enthalpy recovery endotherm observed to the physical aging of the interfacial material of their phase-separated blends.[29]

In Figure 6a, it can clearly be seen that T_{gHP} changes shapes with increasing annealing time. T_{gHP} is found to broaden and at long t_a is observed as an endotherm. As remarked previously the effect of the physical aging of the hard phase is expected to be observed close to its T_g. It is therefore suggested that the change in the aspect of T_{gHP} is due to the appearance and growth of an enthalpy recovery endotherm just below T_{gHP}. The transition observed is thought therefore to correspond to the overlap of T_{gHP} and the associated enthalpy recovery endotherm. As said previously, no enthalpy recovery endotherm is observed for PU-95%HS sample when annealed at 60 °C. The presence of an enthalpy recovery endotherm associated with the hard phase in PU-80%HS sample annealed at 25 °C suggests that the mobility of the hard segments in the hard phase is affected by the presence of the soft segments. It is suggested that the hard segments at the periphery of the hard phase regions in close contact with the soft segments would be more likely to be affected and therefore undergo a relaxation process. This assignment is in agreement with the work of Koberstein et al. on 4,4′-MDI/BDO-based polyurethanes. These authors suggested, based on DSC and thermal mechanical analysis experiments, that the endotherm observed around 80 °C for their system corresponds to a hard phase glass transition event.[28]

When annealing PU-80%HS sample at 60 °C, T_A can clearly be observed around 80 °C as a separate event from T_{gHP} for short annealing times (Figure 6b). Because of the overlap of T_A and T_{gHP} at long annealing times, the choice of a baseline

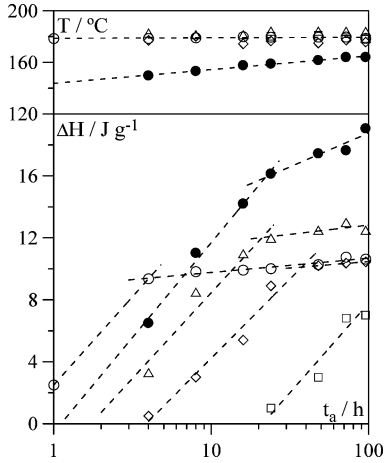

Figure 8. Temperatures and enthalpies of the endotherm $T_{M'} + T_{MMT}$ (see Figure 7) vs the log(t_a) for PU-80%HS sample when annealed at 25 (□), 60 (◇), and 90 °C (△) and temperatures and enthalpies of the endotherm T_M (●) and T_{MMT} (○) (see Figure 7) vs the log(t_a) for PU-80%HS sample when annealed at 120 °C. Upper graph: temperatures. Lower graph: enthalpies.

for measuring the enthalpy associated with T_A affects significantly the values obtained; therefore, the values of ΔH_A at long t_a have not been reported in Figure 7. T_A and ΔH_A are found to increase linearly with log(t_a). In this case again, T_{gHP} is found to broaden slightly and appears as an endotherm for long annealing times (Figure 6b). In this case, it is thought that an enthalpy recovery endotherm corresponding to the physical aging of the hard phase appears around T_{gHP}.

If 90 °C, is used as annealing temperature T_A and T_{gHP} overlap making the measurement of ΔH_A impossible. At long annealing times T_A can clearly be seen just above T_{gHP} and its temperature is found to increase linearly with log(t_a) (Figure 7). The results obtained here are reminiscent of the results obtained by G. Ten Brinke et al. for diblock copolymers of styrene and 2-vinylpyridine. Polystyrene and poly2-vinylpyridine have very close glass transitions 106 and 100 °C respectively. The shapes of the thermograhs around T_{gHP} for our sample when annealed at 90 °C are very similar to the thermographs obtained by these authors for their diblock copolymer when annealed at 91 °C (Figure 6, ref 30). These authors assigned the recovery endotherm observed for their system to the physical aging of the interfacial materials as well as to the physical aging of the two blocks. In the case of fully phase-separated polystyrene/poly2-vinylpyridine blends two clearly separated enthalpy recovery endotherms corresponding to each polymer are observed.[24,30] In our case the enthalpy recovery endotherm observed when annealing PU-80%HS at 90 °C is thought to correspond to the physical aging of the hard phase and the interfacial material with a glass transition higher than 90 °C.

We will discuss now the transitions observed above T_{gHP}. As shown in the previous section an endothermic transition, T_{MMT}, is always observed around 180 °C for all samples at all annealing temperatures (Figure 4). T_{MMT} was assigned to the microphase mixing of the soft and hard segments.[15,16] As expected, T_{MMT} is also observed for PU-80%HS samples (Figure 6). The temperature at which T_{MMT} is observed is roughly the same for all the samples independent of the annealing temperature used, as can be seen from Figure 8. When the sample is annealed below T_{gHP}, an additional endothermic transition is observed as a shoulder at a slightly lower temperature. This transition is thought to be due to the melting of an ordered structure appearing in the phase-separated mesophase hard phase during the phase separation process. In Figure 1, schematic representations of the morphologies of PU-80%HS sample before and after annealing are presented. As can be seen there are two distinct hard segment populations present in the melt-quenched sample prior annealing. Part of the hard segments form the so-called "pure" hard segment phase, which is present at all times i.e.: before and after annealing. The glass transition of this hard phase is close to the glass transition of the pure hard segments, and therefore, their mobility is expected to be similar to the mobility of the hard segments in the PU-95%HS sample. No ordering process of these hard segments is therefore expected when annealing below T_{gHP}. A second population of hard segments is present in the mixed phase. These hard segments are expected to have a higher mobility due to the plasticizing effect of the soft segments. When the sample is annealed, phase separation occurs in the mixed phase resulting in a phase-separated mesophase. During this process the hard segments in the mixed phase have probably a higher enough mobility to be able to order themselves to a certain extent resulting in the presence of a small melting endotherm $T_{M'}$ on the DSC thermograph just below T_{MMT}.

In Figure 8 the enthalpies of ($T_{M'} + T_{MMT}$) endotherm, $\Delta H(T_{M'} + T_{MMT})$, as a function of annealing time are plotted. When annealing at 60 and 90 °C the enthalpy is found after a certain delay time to increase linearly with log(t_a) and then to become roughly constant. The delay time as well as the maximum enthalpy value reached increase with increasing annealing temperature (Figure 8). When annealing at 25 °C, the maximum enthalpy value is not reached within the time scale used in this work. The presence of a delay time before the start of phase separation was also observed in our previous work.[15,16] Hashimoto et al. also observed the presence of a delay time, called "incubation time" by these authors, when investigating the phase separation of polystyrene/polyisoprene diblock copolymers.[31] The enthalpy measured for the ($T_{M'} + T_{MMT}$) transition is related to the absolute degree of phase separation as well as to the level of order present in the phase-separated mesophase hard phase. The results obtained suggest that the two processes are simultaneous and that a maximum degree of phase separation and ordering is reached. The increase in the absolute degree of phase separation with increasing annealing temperature is in agreement with the SAXS results presented in the previous section.

When annealing PU-80%HS above T_{gHP} the hard segments present in the "pure" hard phase will be able to order resulting in the presence on the subsequent DSC thermograph of an additional melting endotherm T_M. A close inspection of the thermograph obtained after 4 h annealing at 120 °C reveals the presence of a shoulder between T_M and T_{MMT} corresponding probably to $T_{M'}$. In this case a deconvolution of T_{MMT} and $T_M + T_{M'}$ was performed assuming that T_{MMT} has a symmetric shape (Figure 6d). The values obtained for $\Delta H(T_M + T_{M'})$ and ΔH_{MMT} are presented in Figure 8. A similar behavior for ΔH_{MMT} is found as when lower annealing temperatures are used. ΔH_{MMT} increases linearly with log(t_a) and becomes constant after 1 h. The maximum value reaches by ΔH_{MMT} cannot be directly compared with the maximum value reached for $\Delta H(T_{M'} + T_{MMT})$. The enthalpy associated with $T_M + T_{M'}$ is found to increase linearly with log(t_a) and as in our previous work a "fast" and a "slow" regimes are observed.[15] With increasing annealing time T_M increases and eventually merges with $T_{M'}$.

It is interesting to compare the thermographs of PU-65%HS sample which after melt-quenching has a single mixed phase morphology and of PU-80%HS sample which has after melt-quenching a two phase morphology consisting of a "pure" hard

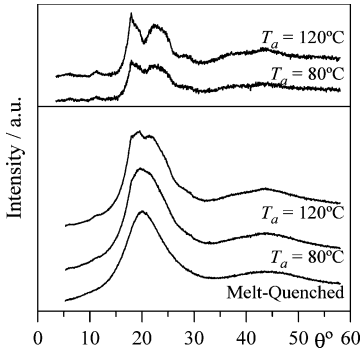

Figure 9. Lower graph: wide-angle X-ray diffracted intensity $I(\theta)$ vs the scattering angle θ for the PU-80%HS sample annealed for 96 h at T_a. Upper graph: wide-angle X-ray diffracted intensity $I(\theta)$ subtracted for amorphous scattering (see text for details) vs the scattering angle θ for the PU-80%HS sample annealed for 96 h at T_a.

segment phase coexisting with a mixed phase with a hard segment content of 65 wt %. In both these samples, the hard segments present in the mixed phase are expected to have a similar mobility. As can be seen from Figures 4 and 6, $T_{M'}$ is observed for both samples at roughly the same temperature when annealed at temperatures bellow T_{gHS}, suggesting the presence of a similar ordered structure in both samples supporting the interpretation made above concerning the origin of $T_{M'}$. When annealed at 120 °C, it is expected that PU-65%HS sample will develop a single melting endotherm at the same temperature as $T_{M'}$ as this sample will present a single hard segment population. This can clearly be seen in Figure 8 of ref 15, where the thermographs obtained for PU-65%HS sample annealed at 120 °C are presented as a function of annealing time. In the case of the PU-80%HS sample as discussed earlier, two distinct hard segment populations are present. When annealed at 120 °C, T_M is found to appear at a lower temperature, roughly 20 °C below $T_{M'}$. This suggests the presence of two separated hard segments population ordering separately.

Some authors have suggested the presence in polyurethanes of different ordered forms resulting in the presence of multiple melting endotherms.[12] In order to verify that the same ordered form is obtained when sample are annealed below and above T_{gHP} WAXS experiments were performed on two PU-80%HS samples annealed at 80 and 120 °C respectively. As can be seen from Figure 9, the level of order in these two samples is very low. In order to be able to compare the two WAXS patterns, the amorphous scattering has been subtracted from the scattering patterns of the two annealed samples. The amount of amorphous scattering subtracted was evaluated so as to obtain a flat resulting curve. The curves presented in Figure 9 were obtained by subtracting 95 and 80% of the scattering curve obtained for the melt-quenched sample (i.e., fully amorphous sample) from the scattering curves obtained for the samples annealed at 80 and 120 °C respectively. As can be seen from Figure 9, the resulting curves are identical suggesting the presence of the same ordered form in both samples. The amount and degree of order reached is function of the annealing temperature and annealing time.

From the results presented in Figure 8 and in our previous work,[15,16] it is reasonable to assume that after 96 h of annealing at temperatures above 25 °C PU-65%HS, PU-75%HS, PU-80%HS, and PU-85%HS samples have reached their maximum degree of phase separation. In our previous work, we showed that when annealed at 120 °C the maximum degree of phase separation (absolute or relative) reached is the same for all the samples.[16] If we assume that this is the case for all the annealing temperatures used then the enthalpy associated with ($T_{M'}$ + T_{MMT}) transition is expected for annealing temperature below T_{gHS} to decrease with increasing hard segment content. $\Delta H(T_{M'} + T_{MMT})$ is indeed expected to be proportional to the amount of phase-separated mesophase present in the sample and the overall amount of phase-separated mesophase present decreases with increasing hard segment content. As can be seem from Table 3 ΔH_{Tot} (=$\Delta H(T_{M'} + T_{MMT})$ for annealing temperatures below T_{gHS}) is found to decrease with increasing hard segment content when 60 and 90 °C are used as annealing temperatures. (The values of $\Delta H(T_{M'} + T_{MMT})$ obtained for the PU-80%HS sample after 96 h annealing at 60 °C is 10.6 J g^{-1}, at 90 °C is 12.5 J g^{-1}, and at 120 °C is 31.2 J g^{-1}). When 120 °C is used as annealing temperature, ΔH_{Tot}, which includes in this case the contribution of T_M, increases with increasing hard segment content. In our previous work we showed that the enthalpy associated with T_{MMT} decreases with increasing hard segment content while the enthalpy associated with T_M and $T_{M'}$ increases.[15]

Conclusion

We have investigated the thermal behavior and the morphological structure of a set of high hard block content polyurethanes. In our previous articles, we have reported on the thermal properties and structure of melt-quenched samples and samples annealed at 120 °C, just above the glass transition of the hard segments T_{gHS}. We have proposed in this earlier work the following morphological model for our samples: after melt-quenching the samples with a hard segment content higher that 65 wt % present a two phase morphology one "pure" hard segment phase coexisting with a mixed (soft + hard segments) phase with a hard segment content of 65 wt %. When the samples are annealed at 120 °C phase separation occurs in the mixed phase resulting in a phase-separated mesophase which has the same structure for all the samples (Figure 1). We were also able to assign the melting endotherms observed at high temperatures to the melting to an ordered structure appearing in the hard segment phase, T_M, and to the microphase mixing of the soft and hard segments, T_{MMT}.

In the present article, we have investigated the origin of the additional endotherms observed when samples are annealed below T_{gHS}. The so-called annealing endotherm, T_A (also called T_1 in the literature), was observed 20−30 °C above the annealing temperature T_a. The temperature and enthalpy of T_A were found to increase linearly with the logarithm of the annealing time t_a. This endotherm was assigned to the relaxation (physical aging) of the interfacial materials with a T_g higher than T_a.

With increasing annealing temperature a change in the appearance of T_{gHP} was observed, and for long annealing times T_{gHP} is observed as an endotherm on the DSC thermographs. The change of shape of T_{gHP} was assigned to the physical aging of the hard phase. It is thought that the presence of the soft segment results in part of the hard segments undergoing some relaxation event below T_{gHP} resulting in an enthalpy relaxation endotherm being present below or around T_{gHP}.

Another additional endotherm, $T_{M'}$, was observed as a shoulder at high temperature, just below T_{MMT}. This endotherm is thought to be due to the ordering of the hard segment present in the mixed phase during the phase separation process. According to the morphological model proposed for a hard segment content higher than 65% two distinct populations of hard segments are expected. Some of the hard segments are residing in the "pure" hard segment phase, and no ordering is expected for these hard segments when annealing temperatures below T_{gHP} are used. Another fraction of the hard segments

resides in the mixed phase. It is suggested that due to the plasticizing effect of the soft segments when phase separation occurs, a certain degree of ordering occurs for these hard segments even when annealed below T_{gHP}, resulting in the presence of a melting endotherm, $T_{M'}$, just below T_{MMT}.

T_{MMT} was observed at all annealing temperatures used, suggesting that, even at low T_a, phase separation occurs. The delay time before phase separation was found to decrease with increasing annealing temperature while the maximum absolute degree of phase separation reached is found to increase with increasing annealing temperature. It seems that a "thermodynamic equilibrium" is reached for each annealing temperature at long enough annealing times. This behavior is consistent with an increase in the mobility of the hard segments with increasing temperature resulting in a higher degree of phase separation.

Acknowledgment. The authors gratefully acknowledge ICI plc for their financial support from their strategic research fund; CRG D2AM for the use of beamline BM02 at ESRF, Grenoble, France; H. Verbeke from Huntsman Polyurethanes, Everberg, Belgium, for the synthesis of the samples; Drs. C. M. Martin and A. J. Gleeson from Daresbury Laboratory, Warrington, U.K., for their support in the use of beamline 16.1 (CCLRC); and J. Shackleton from The University of Manchester for the WAXS measurements.

References and Notes

(1) Woods, G. *The ICI Polyurethanes Book*, 2nd ed.; John Wiley and Sons: New York, 1990.
(2) *Polyurethanes Handbook*; Hanser: Munich, Germany, 1994.
(3) Wilkes, G. L.; Bagrodia, S.; Humphries, W.; Wildnauer, R. *J. Polym. Sci. Part C: Polym. Lett.* **1975**, *13*, 321−327.
(4) Wilkes, G. L.; Emerson, J. A. *J. Appl. Phys.* **1976**, *47*, 4261−4264.
(5) Ryan, A. J.; Macosko, C. W.; Bras, W. *Macromolecules* **1992**, *25*, 6277−6283.
(6) Koberstein, J. T.; Leung, L. M. *Macromolecules* **1992**, *25*, 6205−6213.
(7) Chen, T. K.; Shieh, T. S.; Chui, J. Y. *Macromolecules* **1998**, *31*, 1312−1320.
(8) Phillips, R. A.; Cooper, S. L. *J. Polym. Sci., Part B: Polym. Phys.* **1996**, *34*, 737−749.
(9) Kwei, T. K. *J. Appl. Polym. Sci.* **1982**, *27*, 2891−2899.
(10) Camberlin, Y.; Pascault, J. P. *J. Polym. Sci.: Polym. Chem. Ed.* **1983**, *21*, 415−423.
(11) Chen, T. K.; Chui, J. Y.; Shieh, T. S. *Macromolecules* **1997**, *30*, 5068−5074.
(12) Koberstein, J. T.; Galambos, A. F. *Macromolecules* **1992**, *25*, 5618−5624.
(13) Wilkes, G. L.; Wildnauer, R. *J. Appl. Phys.* **1975**, *46*, 4148−4152.
(14) Chang, Y. J. P.; Wilkes, G. L. *J. Polym. Sci., Part B: Polym. Phys.* **1975**, *13*, 455−476.
(15) Saiani, A.; Daunch, W. A.; Verbeke, H.; Leenslag, J.-W.; Higgins, J. S. *Macromolecules* **2001**, *34*, 9059−9068.
(16) Saiani, A.; Rochas, C.; Eeckhaut, G.; Daunch, W. A.; Leenslag, J. W.; Higgins, J. S. *Macromolecules* **2004**, *37*, 1411−1421.
(17) Leung, L. M.; Koberstein, J. T. *J. Polym. Sci., Part B: Polym. Phys.* **1985**, *23*, 1883−1913.
(18) Roe, R.-J. *Methods of X-Ray and Neutron Scattering in Polymer Science*; Oxford University Press: New York, 2000.
(19) Ruland, W. *J. Appl. Crystallogr.* **1971**, *4*, 70−73.
(20) Bonart, R.; Müller, E. H. *J. Macromol. Sci. Phys.* **1974**, *B10* (1), 177−189.
(21) Guinier, A.; Fournet, G. *Small-Angle Scattering of X-rays*; John Wiley & Sons, Inc.: New York, 1955.
(22) Lagasse, R. R. *J. Appl. Polym. Sci.* **1977**, *21*, 2489−2503.
(23) Hodge, I. M. *J. Non-Cryst. Solids* **1994**, *169*, 211−266.
(24) Tenbrinke, G.; Grooten, R. *Colloid Polym. Sci.* **1989**, *267*, 992−1001.
(25) Chen, H. S.; Wang, T. T. *J. Appl. Phys.* **1981**, *52*, 5898−5902.
(26) Koberstein, J. T.; Stein, R. S. *J. Polym. Sci., Part B: Polym. Phys.* **1983**, *21*, 2181−2200.
(27) Koberstein, J. T.; Stein, R. S. *J. Polym. Sci., Part B: Polym. Phys.* **1983**, *21*, 1439−1472.
(28) Koberstein, J. T.; Galambos, A. F.; Leung, L. M. *Macromolecules* **1992**, *25*, 6195−6204.
(29) Quan, X.; Bair, H. E.; Johnson, G. E. *Macromolecules* **1989**, *22*, 4631−4635.
(30) Tenbrinke, G.; Grooten, R. *Colloid Polym. Sci.* **1989**, *267*, 992−1001.
(31) Hashimoto, T.; Sakamoto, N. *Macromolecules* **1995**, *28*, 4779−4781.
(32) Peebles, L. H. *Macromolecules* **1974**, *7*, 872−882.
(33) Peebles, L. H. *Macromolecules* **1976**, *9*, 58−61.

MA070332P